Auton Robot (2014) 36:67–78
DOI 10.1007/s10514-013-9362-z

Design and control of a three-fingered tendon-driven robotic hand with active and passive tendons

Ryuta Ozawa · Kazunori Hashirii · Yohtaro Yoshimura · Michinori Moriya · Hiroaki Kobayashi

Received: 27 February 2013 / Accepted: 3 August 2013 / Published online: 21 August 2013

Abstract This paper presents a design of a three-fingered robotic hand driven by active and passive tendons and proposes control methods for this hand. The tendon-driven robotic hand consists of the thumb, the index and the middle fingers. The robotic thumb can move all the joints independently. In contrast, the index and the middle robotic fingers are under-actuated using the combination of active and passive tendons, and move the terminal two joints synchronously, which is one of the important features of the human digits. We present passivity-based impedance and force controllers for tendon-driven robotic fingers and discuss how to combine them for fast and secure grasps. We experimentally validate that the robotic hand moves fast and manipulates an object and demonstrate that the robotic hand grasps objects in diverse ways.

Keywords Robotic hand · Tendon-driven mechanisms · Manipulation · Design

R. Ozawa (✉)
Department of Robotics, Ritsumeikan University,
1-1-1 Noji-higashi, Kusatsu, Shiga 535-8577, Japan
e-mail: ryuta@se.ritsumei.ac.jp

K. Hashirii
Research & Development Division, Nabel Co., Ltd., Kyoto, Japan

Y. Yoshimura
Mitsubishi Electric Corporation, Tokyo, Japan

M. Moriya
Construction Machinery Engineering Department,
Kubota Corporation, Osaka, Japan

H. Kobayashi
Department of Mechanical Engineering Informatics, Meiji University,
1-1-1 Higashi-Mita, Tama, Kawasaki, Kanagawa 214-8571, Japan
e-mail: kobayasi@isc.meiji.ac.jp

1 Introduction

Multi-fingered robotic hands have been developed for the last three decades to realize dexterous grasp and manipulation for applications of the outer space, works in daily life and prosthetic hands. These robotic hands are usually designed using small actuators, linkage mechanisms or tendon-driven mechanisms (TDMs).

Small actuators can be mounted in fingers or the palm of robotic hands and makes the hands compact (Kawasaki et al. 2002; Mouri et al. 2011). Therefore, it is easy to install the hand on the robotic arm. However, these actuators limit the grasping force or speed while linkage mechanisms and TDMs can use large actuators to realize large grasping force and speed. Linkage mechanisms are useful in making hands compact but usually limit their motions in a plane (Birglen et al. 2008), except a finger using a special double planetary gear system (Niikura et al. 2011). TDMs make the transmission mechanism complex but can be applied to spatial mechanisms, therefore TDMs have been used to design multi-fingered robotic hands (Jacobsen et al. 1984; Mason and Salisbury 1985; Grebenstein et al. 2010; Bridgwater et al. 2012).

Multi-fingered robotic hands are often designed using fewer actuators than the number of joints to reduce the weight of the hand (Carrozza 2004; Fukaya et al. 2000), or to mimic the anatomical features, especially, kinematic connection between the proximal and distal interphalangeal (PIP/DIP) joints of the digits (Kaneko et al. 2007; Kawasaki et al. 2002). This kinematic connection increases agility of object manipulation when the controllers are appropriately selected (Bae et al. 2005), and helps to passively respond the external forces (Ozawa et al. 2009). The kinematic connection has been realized using the stiff linkage mechanisms (Kaneko et al. 2007; Kawasaki et al. 2002). However, these mechanisms do not

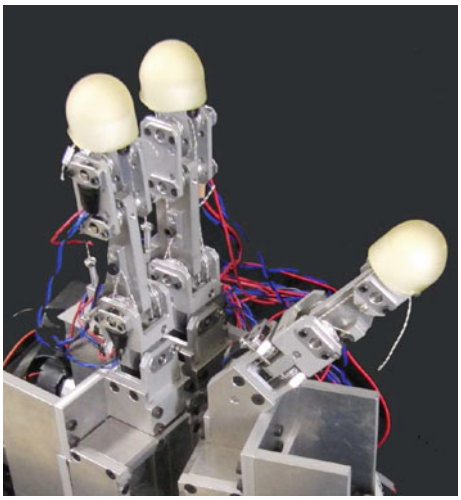

Fig. 1 Three-fingered tendon-driven robotic hand. The *right* robotic finger is the thumb that has three joints driven by four active tendons. The *left* two fingers are the index and the middle fingers that have four joints driven by four active and two passive tendons

respond the external force passively. Hence, elastic mechanisms have been introduced to joints (Carrozza et al. 2006; Liu et al. 1999). These mechanisms are mainly focused on adaptive grasping but are not considered for object manipulation such as pushing or sliding.

In this paper, we develop a new robotic hand and its grasp controllers. First, we present design of a tendon-driven robotic hand, as shown in Fig. 1. This robotic hand consists of modulated motor boxes, full-actuated robotic thumb and two under-actuated fingers. The two under-actuated fingers has two proximal fully actuated degrees of freedom (DOF) and two distal coupled DOFs using the combination of active and passive tendons connected to actuators and elastic elements, respectively. This special coupling is different from the decoupled combination of classical controllability of the fingers with the passive adaptation (Carrozza et al. 2006; Kaneko et al. 2007; Liu et al. 1999, 2007; Lotti et al. 2005), and enables us to design the biomimetic feature of the PIP/DIP joints that move synchronously in free space while they conversely move to absorb the external force in contact tasks. We demonstrate a method to design this special feature based on the tendon kinematic analysis.

Next, we present several grasp controllers for the hand. Recently, postural hand synergies were introduced to analyze a variety of hand motions using the principal component analysis of hand posture (Santello et al. 1998), and have been used to control multiple grasps to combine several principal components of hand posture (Brown and Asada 2007; Catalano et al. 2012). However, it is well known that hand posture is separate from the regulation of the contact force (Santello et al. 1998) and this regulation is important to realize grasps (Johansson and Westling 1984). Therefore, we

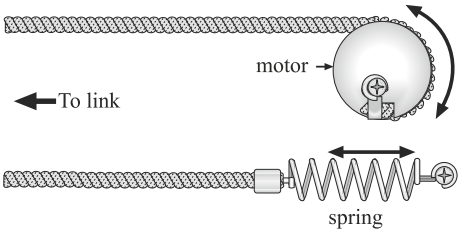

Fig. 2 Active and passive tendons: (*top*) active tendon, (*bottom*) passive tendon

adopt a different approach: we appropriately combine several force and impedance controllers to realize a variety of grasps without any force, tactile and vision sensors. This approach can regulate the internal grasping force and realize fast and secure grasps. For force and impedance controllers of TDMs, several approaches have been proposed using tension sensors (Abdallah et al. 2013; Mason and Salisbury 1985). These methods are very useful for TDMs with sheaths in compensating joint torque errors caused by large friction in sheaths. On the other hand, the developed hand does not use any sheath. Thus, we construct the controllers using the passivity-based approach (Arimoto 1996) because this approach makes it possible to intuitively combine several controllers and to apply the same controllers to both fully-actuated robotic thumb and under-actuated robotic fingers. We present several passivity-based controllers for TDMs and explain how to combine them to realize five different grasps. We experimentally validate the performances of the hand and these controllers.

2 Tendon kinematics and definition of TDMs

First, the basic tendon kinematics is described. Two kinds of tendons are used in the mechanisms; one is an *active tendon* and the other is a *passive tendon*. An active tendon is connected to an actuator, as shown in Fig. 2 (top). The tensile force of an active tendon is determined by the output of the actuator connected to the tendon. It makes no difference if the tendon is rigid or elastic. It is assumed that an active tendon can generate any positive tensile force. A passive tendon is not connected to an actuator, but rather to an elastic element, as shown in Fig. 2 (bottom). The tensile force depends on its deflection. A passive tendon can adjust the pretension, and we assume that the pretension is large enough to prevent the tendons from loosening during operation. Thus, the tensile force is uniquely determined according to the joint configuration.

Let L, M and N be the number of tendons, actuators and joints, respectively, $\boldsymbol{l} \in R^L$ be the deflection of the tendons, $\boldsymbol{q} \in R^N$ be the joint angle vector and $\boldsymbol{\theta} \in R^M$ be the motor angle vector. Then, the following relation is established:

$$\boldsymbol{l} = \begin{bmatrix} \boldsymbol{l}_a \\ \boldsymbol{l}_e \end{bmatrix} = \boldsymbol{J}_j \boldsymbol{q} + \boldsymbol{J}_\theta \boldsymbol{\theta} + \boldsymbol{l}_0$$
$$= \begin{bmatrix} \boldsymbol{J}_a \\ \boldsymbol{J}_e \end{bmatrix} \boldsymbol{q} + \begin{bmatrix} \boldsymbol{R}_\theta \\ \boldsymbol{0} \end{bmatrix} \boldsymbol{\theta} + \begin{bmatrix} \boldsymbol{0} \\ \boldsymbol{l}_{e0} \end{bmatrix}, \quad (1)$$

where $\boldsymbol{J}_j \in R^{L\times N}$ and $\boldsymbol{J}_\theta \in R^{L\times M}$ are Jacobian matrices, $\boldsymbol{l}_0 \in R^L$ is an initial tendon expansion, $\boldsymbol{l}_a \in R^M$ and $\boldsymbol{l}_e \in R^{L-M}$ are the expansion of active and passive tendons, $\boldsymbol{J}_a \in R^{M\times N}$ and $\boldsymbol{J}_e \in R^{(L-M)\times N}$ are Jacobian matrices with respect to the active and the passive tendons. $\boldsymbol{R}_\theta \in R^{M\times M}$ is a diagonal matrix and each diagonal element is the radius of a pulley mounted on a motor axis. The initial expansion of an active tendon is adjustable, thus we assume that it equals zero without loss of generality. On the other hand, an initial expansion of a passive tendon $\boldsymbol{l}_{e0} \in R^{L-M}$ must be positive to prevent the tendon from loosening.

Let tensile force be $\boldsymbol{f}_t$. Using the virtual work principle, the relationship between $\boldsymbol{f}_t \in R^L$ and the joint torque $\boldsymbol{\tau} \in R^N$ is given by:

$$\boldsymbol{\tau} = -\boldsymbol{J}_j^{\mathrm{T}} \boldsymbol{f}_t. \quad (2)$$

Then, the tensile force vector is:

$$\boldsymbol{f}_t = \boldsymbol{A}_1 \boldsymbol{\tau} + \boldsymbol{f}_b = \boldsymbol{A}_1 \boldsymbol{\tau} + \boldsymbol{A}_2 \boldsymbol{\xi}, \quad (3)$$

where

$$\boldsymbol{A}_1 = -\left(\boldsymbol{J}_j^{\mathrm{T}}\right)^+ \text{ and } \boldsymbol{A}_2 = \boldsymbol{I}_L + \boldsymbol{A}_1 \boldsymbol{J}_j^{\mathrm{T}}. \quad (4)$$

$\boldsymbol{f}_b$ is a bias force vector that does not affect $\boldsymbol{\tau}$, and $\left(\boldsymbol{J}_j^{\mathrm{T}}\right)^+$ is the Moore–Penrose pseudo-inverse of $\boldsymbol{J}_j$.

Definition 1 If there exists $\boldsymbol{\xi}$ such that

$$\boldsymbol{f}_b = \boldsymbol{A}_2 \boldsymbol{\xi} > 0, \quad (5)$$

then a mechanism driven by tendons is called a TDM.

TDMs can be classified into the following mechanisms in terms of the ranks of the matrices $\boldsymbol{J}_j$ and $\boldsymbol{J}_a$ (Ozawa et al. 2009):

Definition 2
1. A TDM is called a controllable full-TDM (CF-TDM) if both the ranks of the matrices $\boldsymbol{J}_j$ and $\boldsymbol{J}_a$ equal the number of the joint N.
2. A TDM is called a controllable semi-TDM (CS-TDM) if the rank of the matrix $\boldsymbol{J}_j$ equals N and that of the matrix $\boldsymbol{J}_a$ is less than N.
3. A TDM is called an uncontrollable TDM (U-TDM) if the rank of the matrix $\boldsymbol{J}_j$ is less than N.

CF-TDMs are conventional robotic mechanisms that can drive all the joints independently and CS-TDMs have some joints that move synchronously. U-TDMs are kinds of non-holonomic manipulators that cannot determine the joint configuration uniquely (Suzuki et al. 1996). The controllability of TDMs that was originally proposed in Kobayashi et al. (1998) treated only CF-TDMs because the TDMs have only active tendons. Definition 2 can be considered as the extension of this concept to TDMs with active and passive tendons.

Both CS-TDMs and U-TDMs are used for the design of under-actuated robotic hand to adaptively grasp an object with palm (Hirose and Umetani 1978; Dechev et al. 2001) and are frequently treated without distinction (Birglen et al. 2008). However, the difference between these TDMs is critical to design a robotic hand, e.g., CS-TDMs can grasp an object at the fingertips while U-TDMs cannot. Therefore, we design the thumb robot using a CF-TDM and the index and the middle finger robots using CS-TDMs.

3 Design of tendon-driven robotic fingers

Figure 1 shows the three-fingered tendon-driven robotic hand that realizes some functions of the thumb, the index and the middle fingers. The index and the middle fingers have a symmetric structure and are aligned side-by-side. The thumb is located in front of the index finger with the incline to oppose the middle finger and leans back 45° to grasp an object at an appropriate position. The lengths of the thumb and the digits between the first joint and the fingertip are 93 and 133 mm, respectively, which are almost the same sizes of the human's hand. Each finger uses four actuators that are Maxon DC motors with the power of 11 W for generating more than 50 N tensile forces. As a result, each joint can move about 3 Hz with the peak-to-peak amplitude of 30°, and the finger generates more than 10 N fingertip force.

In the following subsection, we describe the details of the thumb robot and the index and the middle finger robots.

3.1 The thumb robot

Figure 3 shows the photo, kinematics, tendon route and schematic graphs of the thumb robot. The thumb has three joints ($N = 3$). The first two and the third joints correspond to middle phalanx (MP) joints and the interphalangeal (IP) joint of the human's thumb, respectively. The thumb robot must be designed as a CF-TDM that requires at least $N + 1$ actuators to move all the joints independently. Therefore, we used four actuators that are located in a modulated box at the basement. The tendon Jacobian matrix of the thumb robot is designed as follows:

$$\boldsymbol{J}_j = \boldsymbol{J}_a = \begin{bmatrix} r & r & r \\ r & -r & -r \\ -R & R & 0 \\ -R & -R & 0 \end{bmatrix}, \quad (6)$$

where $r = 4.5$ mm and $R = 7.0$ mm. The rank of $\boldsymbol{J}_a$ as well as that of $\boldsymbol{J}_j$ is N in this case, thus this tendon Jacobian matrix $\boldsymbol{J}_j$ satisfies the requirement of a CF-TDM in Definition 2.

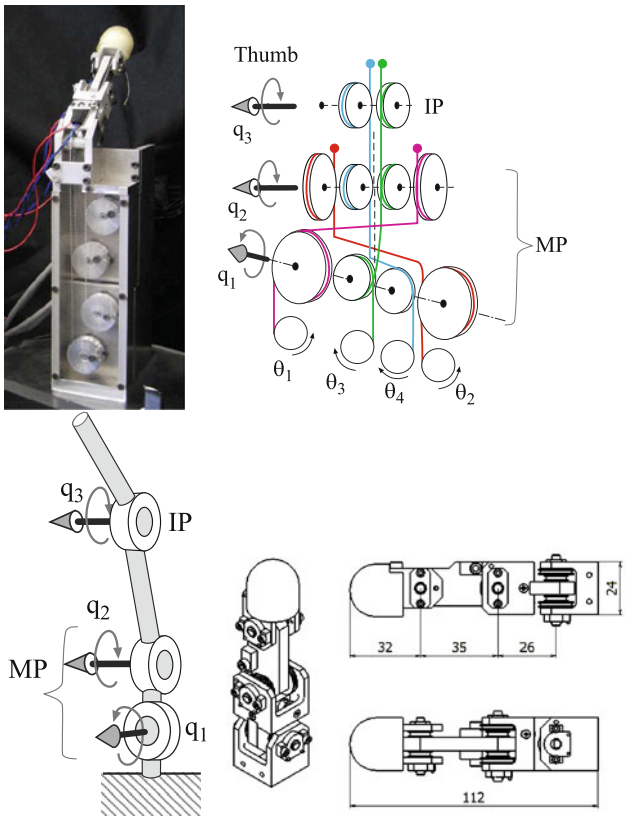

Fig. 3 Thumb robot. (*Top left*) photo, and (*top right*) tendon wiring, (*bottom left*) kinematics and (*bottom right*) the sketches of the thumb robot with the dimensions in millimeter

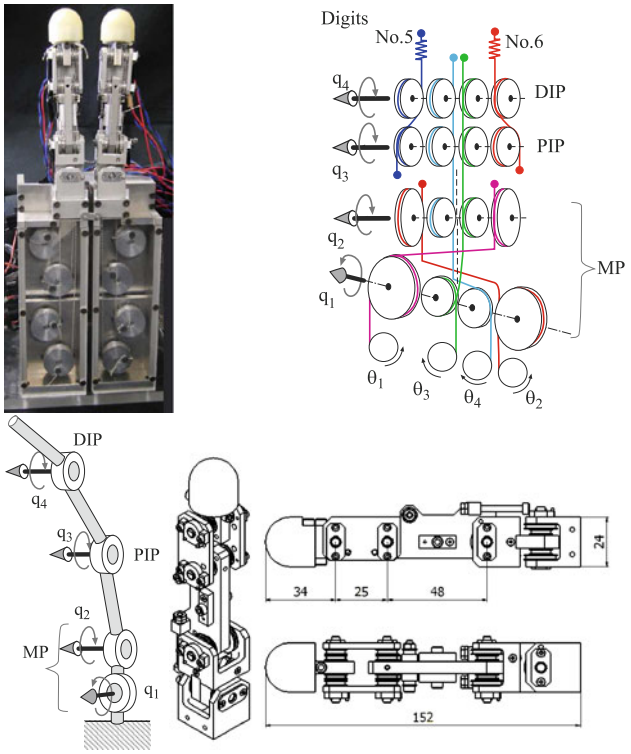

Fig. 4 The index and middle finger robots. (*Top left*) photo of the fingers. The *right* and the *left* are the index and the middle fingers, respectively. (*Top right*) tendon wiring of the index finger. The wiring of the middle finger is symmetric to this. (*Bottom left*) kinematics of the index and the middle fingers. (*Bottom right*) the sketches of the index and the middle fingers with the dimensions in millimeter

3.2 The index and the middle finger robots

The index and the middle fingers are usually modeled as the four joint mechanisms, as shown in Fig. 4 (bottom left). The first two joints are the MP joints to realize the abduction/adduction and curling/extension, respectively. The terminal two joints are DIP/PIP joints to realize curling/extension. When the finger moves in free space, these IP joints move synchronously, as shown in Fig. 5b. This means that the finger uses only one driving DOF for the two joints, i.e., the finger is under-actuated. On the other hand, the finger resists the external force at the fingertip to rotate the DIP joint conversely to the PIP joint when the fingertip contacts with the environment, as shown in Fig. 5c. For the sake of modularity, it is preferable for all fingers to have identical kinematic structure. Therefore, we need to consider the following points to design the index and the middle finger robots:

(i) The finger robots must be CS-TDMs because they are under-actuated and their configuration must be determined uniquely for the external force.
(ii) The DIP and the PIP joints must rotate synchronously if no external force affects.

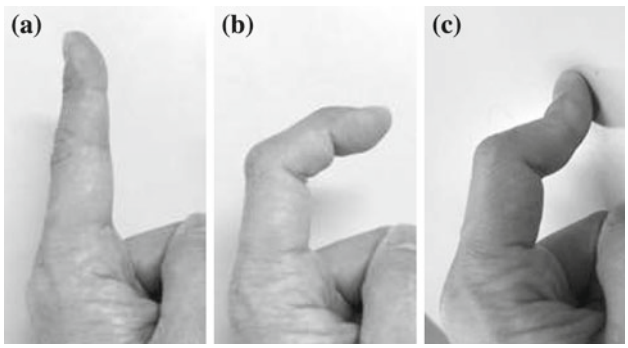

Fig. 5 Connected motion of the DIP and PIP joints **a** normal, **b** free motion, **c** contact motion

(iii) The remaining three DOF, i.e., two MP joints and one of the IP joints of the index and the middle fingers, must be controlled independently.

This feature is realized effectively if control of the remaining DOF does not affect the synchronization of the DIP and the PIP joints, and vice versa.

To make this point clear, we assume that the finger robot is in the equilibrium, the actuators are fixed and the active

and the passive tendons generate tensile forces proportional to the tendon deflection, as follows:

$$\boldsymbol{f}_t = \begin{bmatrix} \boldsymbol{f}_{ta} \\ \boldsymbol{f}_{tb} \end{bmatrix} = \boldsymbol{K}\boldsymbol{J}_j(\boldsymbol{q}-\boldsymbol{q}_0)+\boldsymbol{f}_b = \begin{bmatrix} \boldsymbol{K}_a\boldsymbol{J}_a(\boldsymbol{q}-\boldsymbol{q}_0) \\ \boldsymbol{K}_e\boldsymbol{J}_e(\boldsymbol{q}-\boldsymbol{q}_0) \end{bmatrix} + \begin{bmatrix} \boldsymbol{f}_{ba} \\ \boldsymbol{f}_{be} \end{bmatrix}, \tag{7}$$

where $\boldsymbol{K}$, $\boldsymbol{K}_a$ and $\boldsymbol{K}_e$ are the diagonal stiffness matrices of all the tendons, the active ones and the passive ones, respectively, $\boldsymbol{q}_0$ is the joint angle at the equilibrium, and $\boldsymbol{f}_{ba}$ and $\boldsymbol{f}_{be}$ are the bias force vectors of the active and the passive tendons, respectively. Then, from Eq. (2), the joint torque $\boldsymbol{\tau}$ in the vicinity of the equilibrium point $\boldsymbol{q}_0$ is given as follows:

$$\boldsymbol{\tau} = -\boldsymbol{J}_j^{\mathrm{T}}\boldsymbol{f}_t = -\boldsymbol{J}_j^{\mathrm{T}}\boldsymbol{K}\boldsymbol{J}_j(\boldsymbol{q}-\boldsymbol{q}_0) = -(\boldsymbol{J}_a^{\mathrm{T}}\boldsymbol{K}_a\boldsymbol{J}_a+\boldsymbol{J}_e^{\mathrm{T}}\boldsymbol{K}_e\boldsymbol{J}_e)(\boldsymbol{q}-\boldsymbol{q}_0). \tag{8}$$

To guarantee that $\boldsymbol{q}_0$ is the unique equilibrium point, we need that

$$\operatorname{rank}\boldsymbol{J}_j = N = 4. \tag{9}$$

The relationship between the DIP and PIP joint movements is nearly linear in unconstrained motion (Darling et al. 1994). Therefore, in this design, we assumed that the relationship is linear and the ratio is 1:1. Then, the constraint condition of the DIP and the PIP joints is expressed as follows:

$$\boldsymbol{c}^{\mathrm{T}}\boldsymbol{q} = \begin{bmatrix} 0 & 0 & 1 & -1 \end{bmatrix}\boldsymbol{q} = q_3 - q_4 = 0. \tag{10}$$

Equation (8) indicated that the equilibrium point of TDMs generally depends on both active and passive tendons. This dependency complicates the derivation of the equilibrium point. In addition, the active tendons must generate larger tension to keep the constraint condition (10) than to increase the gripping force. These drawbacks are removed by decoupling the passive tendons from the active tendons.

Therefore, the following relationship must be established among the ranks of these tendon Jacobians:

$$\operatorname{rank}\boldsymbol{J}_j = \operatorname{rank}\boldsymbol{J}_a + \operatorname{rank}\boldsymbol{J}_e = 4. \tag{11}$$

As the passive tendons remain unchanged under the constraint, the following equation must be satisfied:

$$\boldsymbol{J}_e(\boldsymbol{q}-\boldsymbol{q}_0) = \boldsymbol{J}_e\boldsymbol{q} - \boldsymbol{l}_{e0} = 0. \tag{12}$$

Note that $\boldsymbol{l}_{e0}$ can be neglected in the design process because it is adjustable. The IP joint connection is only the constraint in this system. Thus,

$$\operatorname{rank}\boldsymbol{J}_e = 1. \tag{13}$$

Equations (13) and (11) indicate that

$$\operatorname{rank}\boldsymbol{J}_a = 3. \tag{14}$$

Next, to drive the mechanism using the tendons, there exists $\boldsymbol{f}_b > 0$ such that

$$\boldsymbol{J}_j^{\mathrm{T}}\boldsymbol{f}_b = \boldsymbol{J}_a^{\mathrm{T}}\boldsymbol{f}_{ba} + \boldsymbol{J}_e^{\mathrm{T}}\boldsymbol{f}_{be} = 0. \tag{15}$$

As the row vectors of $\boldsymbol{J}_a$ and $\boldsymbol{J}_e$ are linearly independent, Eq. (15) can be rewritten as follows:

$$\boldsymbol{J}_a^{\mathrm{T}}\boldsymbol{f}_{ba} = 0 \text{ and } \boldsymbol{J}_e^{\mathrm{T}}\boldsymbol{f}_{be} = 0. \tag{16}$$

Definition 1 and Eq. (16) indicated that the mechanism driven by only the active tendons or only the passive tendons is an independent TDM. Thus, we can design the finger robots in the following procedure:

Step (1) Design $\boldsymbol{J}_e$ satisfying the following conditions:

(a) $\boldsymbol{J}_e\boldsymbol{q} = 0$ if and only if $\boldsymbol{c}^{\mathrm{T}}\boldsymbol{q} = 0$.
(b) $\operatorname{rank}\boldsymbol{J}_e = 1$ and there exists $\boldsymbol{f}_{be} > 0$ such that $\boldsymbol{J}_e^{\mathrm{T}}\boldsymbol{f}_{be} = 0$.

Step (2) Design $\boldsymbol{J}_a$ satisfying the following conditions:

(c) $\operatorname{rank}\boldsymbol{J}_a = 3$ and there exists $\boldsymbol{f}_{ba} > 0$ such that $\boldsymbol{J}_a^{\mathrm{T}}\boldsymbol{f}_{ba} = 0$.
(d) $\operatorname{rank}\boldsymbol{J}_j = \operatorname{rank}\boldsymbol{J}_a + \operatorname{rank}\boldsymbol{J}_e = 4$.

First, we consider Step (1) for the design of the index finger. We combined Eq. (10) multiplied by the pulley radius r with the symmetric equation to guarantee the existence of $\boldsymbol{f}_{be}$ satisfying Eq. (10) as follows:

$$\boldsymbol{J}_e\boldsymbol{q} = r\begin{bmatrix} \boldsymbol{c}^{\mathrm{T}} \\ -\boldsymbol{c}^{\mathrm{T}} \end{bmatrix}\boldsymbol{q} = \begin{bmatrix} 0 & 0 & r & -r \\ 0 & 0 & -r & r \end{bmatrix}\boldsymbol{q} = 0. \tag{17}$$

$\boldsymbol{J}_e$ satisfies (a) and (b) in Step (1) when we choose $\boldsymbol{f}_{be} = (1,1)^{\mathrm{T}} > 0$.

Next, we consider Step (2). The active tendon Jacobian is designed to drive the remaining DOF independently. The joint motion $\boldsymbol{q} = (q_1, q_2, q_3, q_4)^{\mathrm{T}}$ can be decomposed as follows:

$$\boldsymbol{q} = \boldsymbol{a}_1 + \boldsymbol{a}_2 = \begin{bmatrix} q_1 \\ q_2 \\ \frac{q_3+q_4}{2} \\ \frac{q_3+q_4}{2} \end{bmatrix} + \begin{bmatrix} 0 \\ 0 \\ \frac{q_3-q_4}{2} \\ -\frac{q_3-q_4}{2} \end{bmatrix}. \tag{18}$$

where $\boldsymbol{a}_1$ and $\boldsymbol{a}_2$ are vectors in the nullspace of $\boldsymbol{J}_e$ and in the range space of $\boldsymbol{J}_e^{\mathrm{T}}$, respectively. To guarantee the condition (d) in Step (2), the equation $\boldsymbol{J}_a\boldsymbol{a}_2 = 0$ must be satisfied for any $\boldsymbol{a}_2$. This can be done by choosing the row vectors of $\boldsymbol{J}_a$ from the nullspace of $\boldsymbol{J}_e$. Then, we can use the following $\boldsymbol{J}_a$ to control the remaining DOF:

$$\boldsymbol{J}_a = \begin{bmatrix} r & r & r & r \\ r & -r & -r & -r \\ -R & R & 0 & 0 \\ -R & -R & 0 & 0 \end{bmatrix}. \tag{19}$$

$\boldsymbol{J}_a$ satisfies the condition (c) when we choose $\boldsymbol{f}_{ba} = (R, R, r, r)^{\mathrm{T}} > 0$. Finally, $\boldsymbol{J}_j$ is given as follows:

$$\boldsymbol{J}_j = \begin{bmatrix} \boldsymbol{J}_a \\ \boldsymbol{J}_e \end{bmatrix} = \left[\begin{array}{cccc} r & r & r & r \\ r & -r & -r & -r \\ -R & R & 0 & 0 \\ -R & -R & 0 & 0 \\ \hdashline 0 & 0 & r & -r \\ 0 & 0 & -r & r \end{array}\right]. \tag{20}$$

The index and the middle finger robots are the same structure, but the actuation and the tendon-wiring of the robots are symmetric. These finger robots as well as the thumb robot use four actuators and the first columns of $\boldsymbol{J}_a$ in Eqs. (6) and (19) have the same structure. Therefore, the same actuator boxes can be used as shown in Figs. 3 and 4. Figure 6 focuses on the tendon routes of the IP joints. The two passive tendons cross between the IP joints and two active tendons are aligned parallel. The IP joints synchronously move without changing the length of the passive tendons in free motion (Fig. 6b). On the other hand, when an external force is added to the fingertip, the lengths of passive tendons change and the DIP and PIP joints move in the anti-directions (i.e., the PIP joint rotates in clockwise and the DIP joint rotates in counterclockwise. See Fig. 6c).

Note that many conventional index finger robots have been designed to realize connected IP joint motion, and are classified into two classes; (i) DIP and PIP joints are rigidly connected (Liu et al. 2007; Kaneko et al. 2007) or (ii) joint-independent elastic components are inserted into the joints (Carrozza et al. 2006; Liu et al. 1999; Lotti et al. 2005). The former, the robot with the rigid joints, realizes connected motion in free space, but it is difficult to realize soft contact motion. The latter, the robot with elastic components, can

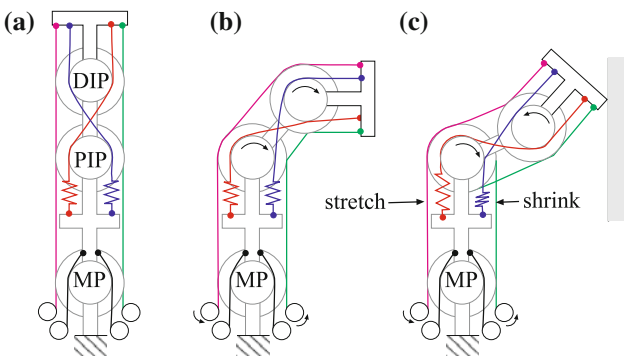

Fig. 6 A passive tendon mechanism to realize the special movements between the DIP and PIP joints **a** normal, **b** free motion, **c** contact motion

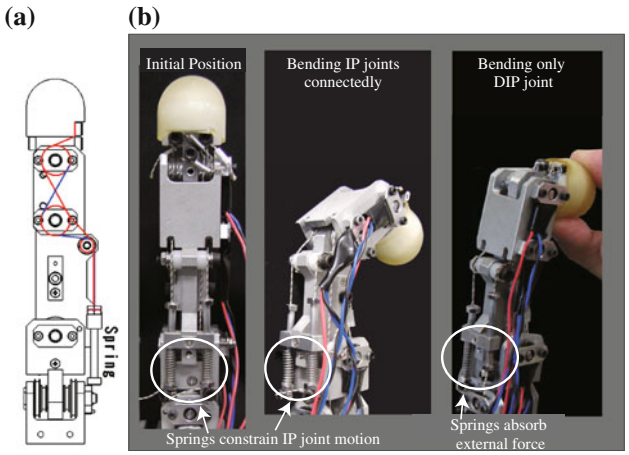

Fig. 7 The spring mechanisms and its effect in the digits. **a** The wire routes of the passive tendons. **b** The effect of the spring mechanism. When the terminal two joints (IP joints) move in free space, the springs keep the lengths and allow the IP joints to move synchronously. In contrast, the springs are shrunken and stretched when the external force is acted on the fingertip

contact softer, but during the contact, all the joints move in the same direction (or only the DIP joint moves). If the finger pushes the environment stronger, then the finger becomes straighter and the contact point moves in the tangential direction. This makes the contact point slippery, and this is undesired motion during pushing operation.

The spring mechanism was designed, as shown in Fig. 7a. The passive tendon depicted as the lines connected from the left bottom of the fingertip to the upper end of the rods where the springs are attached. As shown in Fig. 7b, it was experimentally demonstrated that the length of the springs was not changed from the initial position (left) when the IP joints moved synchronously (middle). In contrast, when an external force is applied to the fingertip, the length was changed to absorb the force.

4 Passivity-based control of TDM

A tendon driven robotic finger consists of rigid-body linkages and actuators connected by tendons. Therefore, the dynamics of the i-th finger is given as follows:

$$\boldsymbol{H}^i \ddot{\boldsymbol{q}}^i + \boldsymbol{d}_q^i + \boldsymbol{g}_q^i + (\boldsymbol{J}_j^i)^{\mathrm{T}} \boldsymbol{f}_t^i = \boldsymbol{0}, \tag{21}$$

$$\boldsymbol{H}_\theta^i \ddot{\boldsymbol{\theta}}^i + \boldsymbol{B}_\theta^i \dot{\boldsymbol{\theta}}^i + (\boldsymbol{J}_\theta^i)^{\mathrm{T}} \boldsymbol{f}_t^i = \boldsymbol{\tau}_a^i. \tag{22}$$

The superscript i is used to distinguish the fingers and we assign $i = 1, 2, 3$ for the thumb, index and middle fingers, respectively. $\boldsymbol{H}^i$ and $\boldsymbol{H}_\theta^i$ are the inertia matrices of the robot and the motors, respectively, $\boldsymbol{d}_q^i$ and $\boldsymbol{g}_q^i$ are the Coriolis and centrifugal force and the gravitational force of the links, $\boldsymbol{B}_\theta^i$ is the damping matrices of the motor and $\boldsymbol{\tau}_a^i$ is the motor

torque vector. The first and second equations are the dynamics of the finger linkages and the motors, respectively. The motor dynamics is connected to the link dynamics through the active tendons. The elastic force generated by the passive tendons affects only on the linkages. The control problem is how to design the control input $\boldsymbol{\tau}_a = (\boldsymbol{\tau}_a^1, \boldsymbol{\tau}_a^2, \boldsymbol{\tau}_a^3)$ for the full-actuated thumb and the under-actuated fingers. PI controllers were frequently used for tendon-driven robotic fingers with sheaths to cope with large friction (Mason and Salisbury 1985; Abdallah et al. 2011). However, the designed hand does not use any sheath in the transmission. Therefore, we use passivity-based impedance and force controllers for fingers and combine them to realize selected grasps.

4.1 Joint space impedance control of TDMs

This subsection presents the joint space impedance controller (Ozawa et al. 2009). Let $\boldsymbol{q}_d^i$ be the desired joint angle of the i-th finger. Then we can define the corresponding motor angle $\boldsymbol{\theta}_d^i$ as follows:

$$\boldsymbol{\theta}_d^i = -(\boldsymbol{R}_\theta^i)^{-1} \boldsymbol{J}_a^i \boldsymbol{q}_d^i \tag{23}$$

For the convergence of $\boldsymbol{q}^i$ on $\boldsymbol{q}_d^i$, we design a controller as follows:

$$\boldsymbol{\tau}_{a0}^i = -\boldsymbol{K}_p^i \Delta\boldsymbol{\theta}^i - \boldsymbol{K}_v^i \dot{\boldsymbol{\theta}}^i + (\boldsymbol{J}_\theta^i)^{\mathrm{T}} \left\{ \boldsymbol{A}_1^i \boldsymbol{g}_q^i + \boldsymbol{f}_b^i \right\}, \tag{24}$$

where $\boldsymbol{K}_p^i$ and $\boldsymbol{K}_v^i$ are the positive definite matrices, $\Delta\boldsymbol{\theta}^i = \boldsymbol{\theta}^i - \boldsymbol{\theta}_d^i$ and $\boldsymbol{f}_b^i$ is the bias force. In general, the bias force is determined by using a constant value which is adequately large, by solving optimization problems (Mason and Salisbury 1985; Ma et al. 1993; Abdallah et al. 2013) or by determining the passive joint compliance (Kobayashi et al. 1998). We adopt the constant bias force for the hand thanks to the large actuator power. However, we can use any of them except (Kobayashi et al. 1998) because this controller does not depend on bias force algorithms.

Note that the thumb robot can freely choose the desired joint angle $\boldsymbol{q}_d^i$, while the desired angle of the index and the middle finger robots is restricted because of the under-actuation. Let $\hat{\boldsymbol{q}}_d^i$ be the nominal desired joint position, which is designed by an operator. If the passive tendons play role of joint constraints, a desired joint angle $\boldsymbol{q}_d^i$ should be calculated from a nominal desired joint angle $\hat{\boldsymbol{q}}_d^i = (\hat{q}_{d1}^i, \hat{q}_{d2}^i, \hat{q}_{d3}^i, \hat{q}_{d4}^i)$ as follows:

$$\boldsymbol{q}_d^i = \begin{cases} \hat{\boldsymbol{q}}_d^i & \text{for thumb,} \\ \boldsymbol{P}_e^i \hat{\boldsymbol{q}}_d^i = \left(\hat{q}_{d1}^i \;\; \hat{q}_{d2}^i \;\; \frac{\hat{q}_{d3}^i + \hat{q}_{d4}^i}{2} \;\; \frac{\hat{q}_{d3}^i + \hat{q}_{d4}^i}{2} \right)^{\mathrm{T}} & \text{otherwise,} \end{cases} \tag{25}$$

where $\boldsymbol{P}_e^i = \boldsymbol{I} - (\boldsymbol{J}_e^i)^+ \boldsymbol{J}_e^i$, where $(\boldsymbol{J}_e^i)^+$ is a the Moore-Penrose pseudo-inverse of $\boldsymbol{J}_e^i$.

4.2 Taskspace control of TDMs

The taskspace controller is used to control the position and force described in the task space. In the joint space control, we needed to take the joint constraint into account for the joint motion planning. In contrast, in the force control, we do not need to consider about the joint constraint, because each finger have three actuated DOF that are equivalent to the dimensions of the force. The desired force depends on tasks. In this paper, we design three taskspace controllers for positioning, pushing and pinching. To realize a desired force, we control the desired joint torque $\boldsymbol{\tau}_{\mathrm{task}k}^i$ $(k = 1, 2, 3)$ using the following motor torque controller:

$$\boldsymbol{\tau}_{ak}^i = -\boldsymbol{K}_v^i \dot{\boldsymbol{\theta}}^i + (\boldsymbol{J}_\theta^i)^{\mathrm{T}} \left[\boldsymbol{A}_1^i \left\{ \boldsymbol{g}_q^i + \boldsymbol{\tau}_{\mathrm{task}k}^i \right\} + \boldsymbol{f}_b^i \right], \tag{26}$$

where $\boldsymbol{K}_v^i$ is the feedback gain. The first term of Eq. (26) gives the motor damping, and the second term is for the gravity compensation, one of the following task controllers and the bias force. In the following subsection, we design the desired torque $\tau_{\mathrm{task}k}^i$.

4.2.1 Impedance controller

A taskspace impedance controller that regulates a position $\boldsymbol{s}^i \in R^3$ of the fingertips in the taskspace to the desired one $\boldsymbol{s}_d^i$ is given as follows:

$$\boldsymbol{\tau}_{\mathrm{task1}}^i = -(\boldsymbol{J}_s^i)^{\mathrm{T}} \boldsymbol{K}_s^i \Delta\boldsymbol{s}^i, \tag{27}$$

where $\boldsymbol{J}_s^i = \frac{\partial \boldsymbol{s}^i}{\partial \boldsymbol{q}^i}$ and $\Delta\boldsymbol{s}^i = \boldsymbol{s}^i - \boldsymbol{s}_d^i$. Unlike the joint impedance controller, the dimension of the fingertip position $\boldsymbol{s}^i$ is three, which is equivalent to the driving DOF of the fingers. Therefore, the joint configuration $\boldsymbol{q}^i$ corresponding to the position $\boldsymbol{s}^i$ is uniquely determined.

4.2.2 Force controller

When we would like to have the finger scratch or slide an object, we must control the endpoint force in the normal direction to the environment. Then, we use the following force controller (Ozawa and Moriya 2010):

$$\boldsymbol{\tau}_{\mathrm{task2}}^i = -(\boldsymbol{J}_s^i)^{\mathrm{T}} \left\{ \boldsymbol{K}_s^i \boldsymbol{S}_p^i \Delta\boldsymbol{s}^i + \boldsymbol{S}_f^i \boldsymbol{f}_d^i \right\}, \tag{28}$$

where $\boldsymbol{S}_p^i$ and $\boldsymbol{S}_f^i$ are the selection matrices that determine the position-controlled and force-controlled directions, respectively, $\boldsymbol{f}_d^i \in R^3$ are the desired contact force. This position controller is feedback but the force controller is feedfoward. Therefore, this controller does not suitable for accurately track a desired contact force. However, many operations used in hand such as sliding and pushing an object usually do not require precise tracking of the contact force. Thus, we do not adopt a force feedback controller in this paper. If the force

feedback is needed for application, we can modified it by adding the force sensor at the fingertip and the integral term of the force error to Eq. (28).

4.2.3 Blind grasping controller

The blind grasping controller is designed for pinching an object and is defined as follows (Ozawa et al. 2005):

$$\boldsymbol{\tau}^i_{\text{task3}} = -k^i_p (\boldsymbol{J}^i_s)^{\mathrm{T}} (\boldsymbol{x}^i - \boldsymbol{x}^j), \tag{29}$$

where k^i_p is the feedback gain, $\boldsymbol{x}^i$ is the position of the i-th fingertip and $\boldsymbol{x}^j$ is that of an opposed finger or the opposed thumb. This controller is similar to the taskspace impedance controller (27) but the error vector is different. The taskspace in the impedance and force controllers may depend on the environment, but the fingertip position does not depend on the environment and can be described in the local hand coordinates. The error vector $\boldsymbol{x}^i - \boldsymbol{x}^j$ expresses the opposed direction between the thumb and one of the remaining digits. k^i_p corresponds to one-dimensional spring between the fingertips, thus k^i_p is scalar. This controller drastically improves the stability of the pinching motion.

4.3 Grasping controllers

We can realize several hand motions by combining the above joint and task-space controllers. From Cutokosky's taxonomy (Cutkosky 1989) we selected five different grasps to manipulate a variety of objects as follows:

1. Envelope grasp,
2. two-fingered precision grasp,
3. three-fingered precision grasp,
4. adducted thumb, and
5. lateral grasp.

Envelope grasp is used to grasp a heavy object with palm. Two-fingered and three-fingered precision grasps are used to pinch a small object with the fingertips and to manipulate it. Lateral grasp is used to pinch a thin object such as paper and a key with the side of the index finger and the fingertip. Adducted thumb is used to grasp a stick-shaped object such as a screw driver and an umbrella.

Envelope grasp requires all the joints in the fingers to close gradually until the palm and the fingers are firmly contact with a grasped object. Therefore, we use only the joint space impedance controller $\boldsymbol{\tau}_a = (\boldsymbol{\tau}^1_{a0}, \boldsymbol{\tau}^2_{a0}, \boldsymbol{\tau}^3_{a0})$.

Two-fingered precision grasp requires the thumb and the index finger to oppose each other and the middle finger to keep an appropriate configuration. Thus, this motion is realized using the blind grasping controller for the thumb and the index finger and the joint impedance controller for the middle finger, thus $\boldsymbol{\tau}_a = (\boldsymbol{\tau}^1_{a3}, \boldsymbol{\tau}^2_{a3}, \boldsymbol{\tau}^3_{a0})$. In contrast, three-fingered grasp is realized only the blind grasping controller $\boldsymbol{\tau}_a = (\boldsymbol{\tau}^1_{a3}, \boldsymbol{\tau}^2_{a3}, \boldsymbol{\tau}^3_{a3})$.

Adducted thumb is similar to the envelope grasp. However, the motion of the thumb is different from that in the case of envelope grasp. In this case we consider a virtual stick that the fingers roll up and that the thumb pushes. To roll up the stick, the fingers are controlled by the joint impedance controller. The thumb is controlled by the task-space impedance controller to press the fingertip on a point in the longitude axis of the virtual stick. Thus, the controller is given as $\boldsymbol{\tau}_a = (\boldsymbol{\tau}^1_{a1}, \boldsymbol{\tau}^2_{a0}, \boldsymbol{\tau}^3_{a0})$.

Lateral grasp consists of two processes: preshaping and pinching. First, all the joints in the digits bend adequately and the thumb move to the side of the index finger for preshaping. Then, the fingertip of the thumb puts on the side of the index finger to pinch an object. Therefore, in the first process, the joint-space impedance controller $\boldsymbol{\tau}_a = (\boldsymbol{\tau}^1_{a0}, \boldsymbol{\tau}^2_{a0}, \boldsymbol{\tau}^3_{a0})$ is used for all the fingers and the thumb. Then, the controller is switched to $\boldsymbol{\tau}_a = (\boldsymbol{\tau}^1_{a2}, \boldsymbol{\tau}^2_{a0}, \boldsymbol{\tau}^3_{a0})$, where the joint-space impedance controllers are used for the digits while the task-space force controller is used for the thumb.

5 Experiment

First, we executed two basic experiments to validate the joint impedance and the force controllers. Next, we combined the task-space and the joint impedance controller to implement several grasps.

Figure 8 shows the first and the second joint motion of the index finger robot in the experiment, where the index finger kept the angle of the first joint unchanged while it moved the rest of the joints to track the sinusoidal function. The joint peak-to-peak amplitude gradually varied between 50 and 30° and the period gradually changed between 2.0 and 0.3 s. The first joint almost kept the angle although the active tendons are kinematically coupled among all the joints. The residual error caused by the friction between the tendons and pulleys and by the unmodeled tendon stretch. The second joint tracked the desired motion until 6.5 s where the time period was about 0.6 s. After 6.5 s, the joint still moved quickly although the overshoot appeared because of the inertial force of the finger.

Figure 9 shows the photo of this experimental setting for the pushing and pulling task and the fingertip position in the horizontal(x) direction. In this experiment, the index finger was controlled by the controller (28) to track $x(t) = 0.015 \sin(4\pi t) + 0.075$ m and to push the object with $f_d = 4$ N. The fingertip tracked the desired position with the response delayed by about 0.1 s, as shown in Fig. 9b. When the finger pulled the object, the passive tendon on the near side was compressed to absorb the external

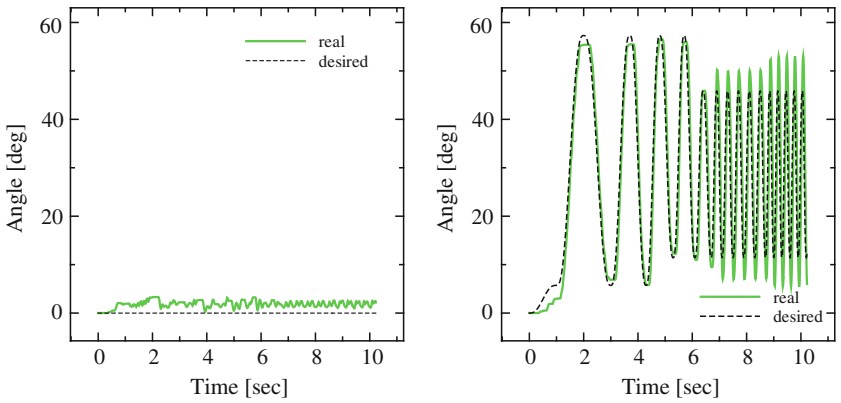

Fig. 8 The trajectory of the first and second joints of the index finger. The desired angle of the first joint is constant, as shown in the *left*. In contrast, the second joint motion in the right is given as a sinusoidal function, whose peak-to-peak amplitude gradually varied between 50 and 30° and whose period gradually changed between 2.0 and 0.3 s

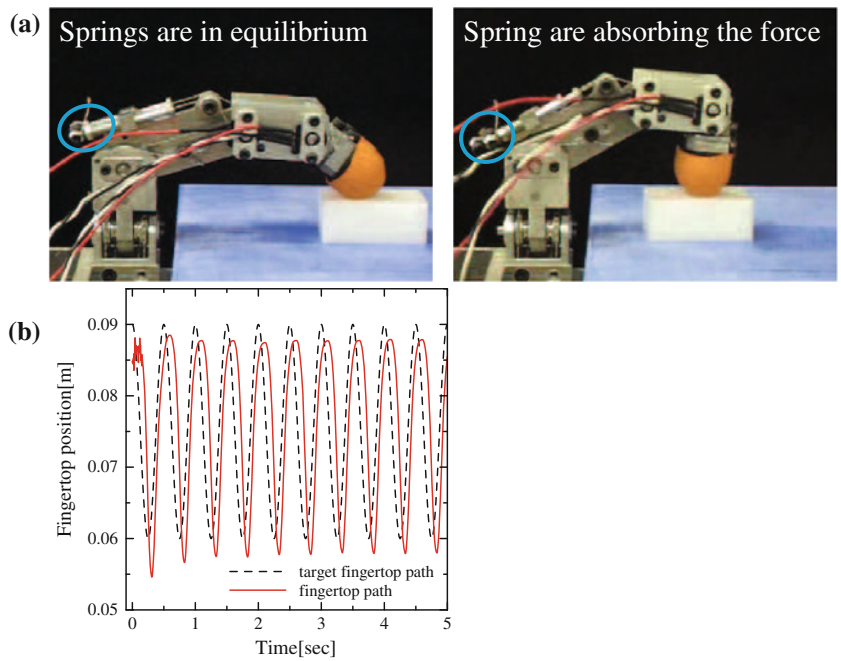

Fig. 9 Pushing and pulling an object using the index finger robot. **a** The photo during the experiment. **b** The endpoint trajectory in the horizontal direction

force, as shown in Fig. 9a. More detail results about sliding manipulation have been reported in Ozawa and Moriya (2010).

Figure 10 shows the snapshots of the five grasps. Two-fingered and three-fingered precision grasps, envelope grasp and adducted thumb were captured in 10 Hz. In contrast, lateral grasp was captured in 5 Hz because this grasp consists of the two actions: preshaping and pinching. In each grasp, a helper manually placed an object between the fingertips and then the robotic hand moved to grasp it. As shown in Fig. 10, the hand reached to the final shapes within four flames after moving, and kept grasping the object after a helper released it. Therefore, the hand realized fast and secure grasps with the combination of the joint and task-space impedance controllers.

6 Conclusion

In this paper, we designed a robotic hand and its controllers. We presented the basic kinematics of the TDMs with active and passive tendons. Based on the kinematics we developed the three-fingered robotic hand which consists of the thumb, the index and the middle fingers. The terminal two joints of the index and the middle fingers were designed using the cross-coupled passive tendons to realize the connected IP joint motion. We confirmed that the passive tendon mechanisms in the index and the middle fingers worked as a constraint in the free motion and absorbed the external force in a constraint motion. In the robotic fingers, we used the linear spring for these passive tendon mechanisms. In contrast, we adjust the stiffness of the corresponding tendons to suit for

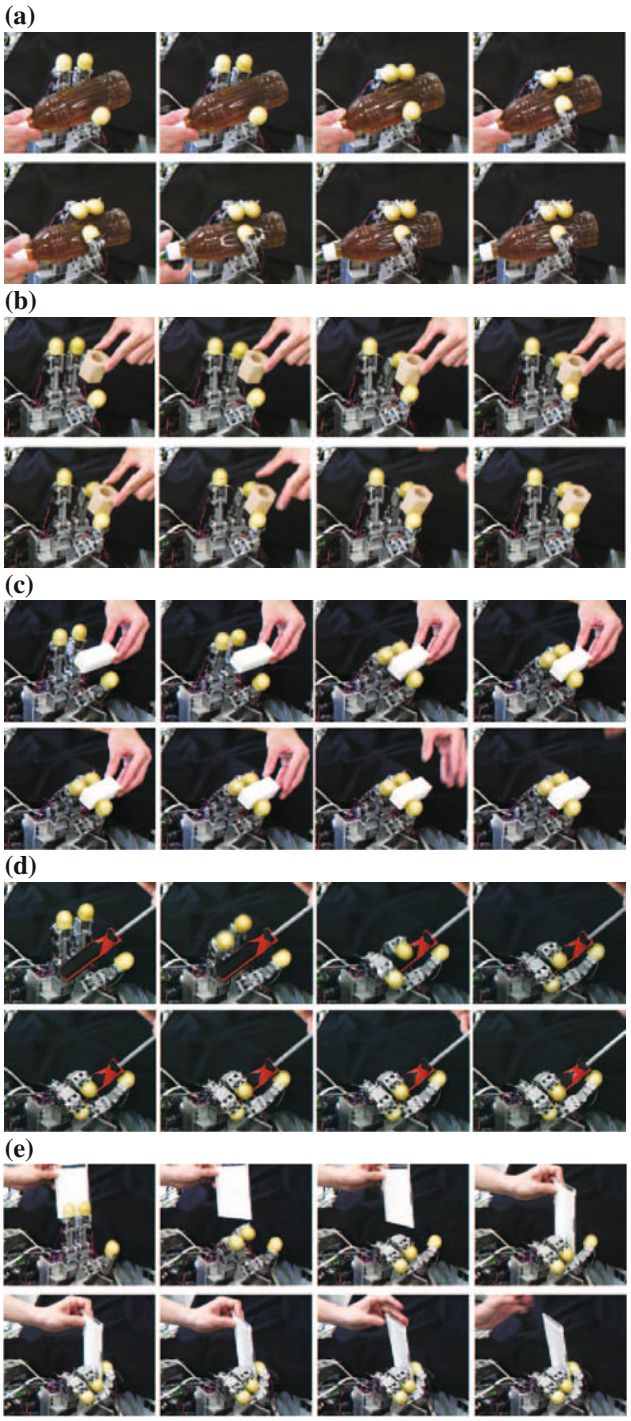

Fig. 10 Object manipulation. **a** Envelope grasp, **b** two-fingered precision grasp, **c** three-fingered precision grasp, **d** adducted thumb and **e** lateral grasp. Each snapshot flows from the *top left* to the *bottom right*. **a**–**d** are captured in 10 Hz, and **d** is captured in 5 Hz

operations in our daily life. We will investigate the non-linear passive tendon mechanisms for fingers and design it.

The developed robotic fingers are almost same size of our fingers, but the actuation boxes are still large. We will improve the size and weight of the hand systems to mount on robotic arms or to use it as a prosthetic hand. We also presented passivity-based controllers for the fingers and combined them to realize five grasps. Experiment validated that the developed robotic hand moved about 3 Hz with the peak-to-peak amplitude of 30° in free space using the joint space impedance controller. The index finger robot slid an object in 2 Hz using the force controller. The passive stiffness of the finger smoothly absorbed the disturbances during the sliding. We also demonstrated that the robotic hand fast and securely grasped a variety of objects using five different grasps without any external sensors. These grasps are useful in some tasks in our daily life. However, these controllers cannot adaptively control the grasping force, which is important, e.g., to grasp a slippery object (Johansson and Westling 1984). In addition, we still need more controllers for executing tasks in our daily life. Therefore, we will develop more controllers and increase the grasping ability.

References

Abdallah, M. E., Platt R. Jr., Hargrave, B., & Permenter, F. (2011). Position control of tendon-driven fingers with position controlled actuators. In *IEEE international conference on robotics and automation, Saint paul, MN* (pp. 2859–2864).

Abdallah, M. E., Platt, R, Jr., & Wampler, C. W. (2013). Decoupled torque control of tendon-driven fingers with tension management. *The International Journal of Robotics Research*, *32*(2), 247–258.

Arimoto, S. (1996). *Control theory of non-linear mechanical systems: A passivity-based and circuit-theoretic approach*. Oxford: Oxford University Press.

Bae, J. H., Arimoto, S., & Yoshida, M. (2005). Control and dexterity in robotic pinching under linking of movements of joints like human fingers. In *Proceedings of the first international conference on complex medical engineering, Takamatsu, Japan* (pp. 899–903).

Birglen, L., Laliberte, T., & Gosselin, C. (2008). *Underactuated robotic hands, Springer tracts in advance robotics* (Vol. 40). Berlin: Springer.

Bridgwater, L., Ihrke, C., Abdallah, M., Radford, N., Rogers, J., Yayathi, S., Askew, R., & Linn, D. (2012). The robonaut 2 hand. In *IEEE international conference on robotics and automation, Saint Paul, MN* (pp. 3425–3430).

Brown, C. Y. & Asada, H. H. (2007). Inter-finger coordination and postural synergies in robot hands via mechanical implementation of principal components analysis. In *Proceedings of IEEE/RSJ international conference on intelligent robots and systems, San Diego, CA* (pp. 2877–2882).

Carrozza, M. C. (2004). The SPRING hand: Development of a self-adaptive prosthesis for restoring natural grasping. *Autonomous Robots*, *16*, 125–141.

Carrozza, M. C., Cappiello, G., Micera, S., Edin, B. B., Beccai, L., & Cipriani, C. (2006). Design of a cybernetic hand for perception and action. *Biological Cybernetics*, *95*, 629–644.

Catalano, M., Grioli, G., Serio, A., Farnioli, E., Pazza, C., & Bicchi, A. (2012). Adaptive synergies for a humanoid robot hand. In *IEEE-RAS international conference on humanoid robots, Osaka, Japan* (pp. 7–14).

Cutkosky, M. R. (1989). On grasp choise, grasp models, and the design of hands for manufacturing tasks. *IEEE Transactions on Robotics and Automation*, *5*(3), 269–279.

Darling, W. G., Cole, K. J., & Miller, G. F. (1994). Coordination of index finger movements. *Journal of Biomechanics*, *27*(4), 479–491.
Dechev, N., Cleghorn, W., & Naumann, S. (2001). Multiple finger passive adaptive grasp prosthetic hand. *Mechanism and Machine Theory*, *36*, 1157–1173.
Fukaya, N., Toyama, S., Asfour, T., & Dillmann, R. (2000). Design of the tuat/karlsruhe humanoid hand. In *Proceedings 2000 IEEE/RSJ international conference on intelligent robots and systems* (pp. 1754–1759).
Grebenstein, M., Chalon, M., Hirzinger, G., & Siegwart, R. (2010). Antagonistically driven finger design for the anthropomorphic DLR hand arm system. In *Proceedings of IEEE international conference on intelligent robots and systems, Taipei, Taiwan* (pp. 609–616).
Hirose, S. & Umetani, Y. (1978). The development of soft gripper for the versatile robothand. *Mechanism and Machine Theory*, *13*, 351–359.
Jacobsen, S. C., Wood, J. E., Knutti, D. F., & Biggers, K. B. (1984). The UTAH/M.I.T. dextrous hand: Work in progress. *The International Journal of Robotics Research*, *3*(4), 21–50.
Johansson, R. & Westling, G. (1984). Roles of glabrous skin receptors and sensorimotor memory in automatic control of precision grip when lifting rougher or more slippery objects. *Experimental Brain Research*, *56*, 550–564.
Kaneko, K., Harada, K., & Kanehiro, F. (2007). Development of multi-fingered hand for life-size humanoid robots. In *Proceedings of IEEE international conference on robotics and automation, Roma, Italy* (pp. 913–920).
Kawasaki, H., Komatsu, T., & Uchiyama, K. (2002). Dexterous anthropomorphic robot hand with distributed tactile sensor: Gifu hand II. *IEEE/ASME Transactions on Mechatronics*, *7*(3), 296–303.
Kobayashi, H., Hyodo, K., & Ogane, D. (1998). On tendon-driven robotic mechanisms with redundant tendons. *The International Journal of Robotics Research*, *17*(5), 561–571.
Liu, H., Butterfass, J., Knoch, S., Meusel, P., & Hirzinger, G. (1999). A new control strategy for DLR's multisensory articulated hand. *IEEE Control Systems Magazine*, *15*, 105–110.
Liu, H., Meusel, P., Seitz, N., Willberg, B., Hirzinger, G., Jin, M. H., et al. (2007). The modular multisensory DLR-HIT-hand. *Mechanism and Machine Theory*, *42*, 612–625.
Lotti, F., Tiezzi, P., Vassura, G., Biagiotti, L., Palli, G., & Melchiorri, C. (2005). Development of ub hand 3: Early results. In *Proceedings of IEEE international conference on robotics and automation, Barcelona, Spain* (pp. 4488–4493).
Ma, S., Hirose, S., & Yashinada, H. (1993). Design and experiments for a coupled tendon-driven manipulator. *IEEE Control Systems Magazine, 13*, 30–36.
Mason, M. T. & Salisbury, J. K. (1985). *Robot hands and the mechanics of manipulation*. Cambridge: The MIT Press.
Mouri, T., Endo, T., & Kawasaki, H. (2011). Review of gifu hand and its application. *Journal of Mechanics*, *39*, 210–228.
Niikura, R., Kunugi, N., & Koganezawa, K. (2011). Developement of artificial finger using the double planetary gear system. In *Proceedings of IEEE/ASME international conference on advanced intelligent mechatronics, Budapest, Hungary* (pp. 481–486).
Ozawa, R., Arimoto, S., Nakamura, S., & Bae, J. H. (2005). Control of an object with parallel surfaces by a pair of finger robots without object sensing. *IEEE Transactions on Robotics*, *21*(5), 965–976.
Ozawa, R., Hashirii, K., & Kobayashi, H. (2009). Design and control of underactuated tendon-driven mechanisms. In: *Proceedings of IEEE international conference on robotics and automation, Kobe, Japan* (pp. 1522–1527).
Ozawa, R. & Moriya, M. (2010). Effects of elasticity on an under-actuated tendon-driven robotic finger. In *Proceedings of IEEE international conference on robotics and biomimmetics, Tianjin, China* (pp. 891–896).
Santello, M., Flanders, M., & Soechting, J. F. (1998). Postural hand synergies for tool use. *The Journal of Neuroscience, 18*(23), 10105–10115.
Suzuki, T., Koinuma, M., & Nakamura, Y. (1996). Chaos and nonlinear control of nonholonmic free-joint manipulator. In *Proceedings of the IEEE international conference on robotics and automation* (pp. 2668–2675).

Ryuta Ozawa received his Ph.D degrees in Mechanical Engineering from Meiji University in 2001. From 2001 to 2002 he was a research assistant at Meiji University. From 2002 to 2003 he was a post-doctoral research fellow of the Japan Society for the Promotion of Science. He joined the department of robotics, Ritsumeikan University in 2003. From 2008 to 2009 he was a visiting scholar at IRISA/INRIA, Rennes, France. He is currently an associate professor at the department of robotics, Ritsumeikan University. He was awarded the encouraging prize for young researchers from the department of System Integration in the Society of Instrument and Control Engineers (SICE) of Japan in 2006, the best paper award from the Robotics Society of Japan in 2007, the outstanding paper prize from the Society of Instrument and Control Engineers of Japan in 2009. He is a member of the IEEE, SICE, ISCIE and the Robotics Society of Japan. His research interests are manipulation of robotic hands and robotic arm, teleoperation of robotic hands, full-actuated/under-actuated tendon-driven robotic arm, mass estimation with a variable stiffness device in micro gravity, balance control of a biped and so on.

Kazunori Hashirii was born in 1984. He received his BS and ME degrees in robotics and computer science from Ritsumeikan University, in 2007 and 2009, respectively. He has worked for Nabel Co., Ltd, Japan, since 2009 and he is currently a leader of the R&D division of the mechanical design group.

Yohtaro Yoshimura received his BE and ME degree in robotics and mechanical engineering from Ritsumeikan University, Japan, in 2010 and 2012, respectively. He is currently working as a software developer of the head unit in Mitsubishi Electric Corporation, Japan.

Michinori Moriya received his BE and ME degree in robotics and mechanical engineering from Ritsumeikan University, in 2007 and 2009, respectively. He is currently working as an engineer in the construction machinery engineering department, Kubota Corporation. His interest is the design of backhoes.

Hiroaki Kobayashi received the BE, ME, and Ph.D. degrees in precision engineering in 1971, 1973, and 1977, respectively, all from Kyoto University. Since 1976 he has been with the School of Science and Technology at Meiji University, Japan, where he is currently a Professor. From 1988 to 1989, he was a postdoctoral fellow in Computer Information Science at the School of Engineering and Applied Science, University of Pennsylvania. His research interests are in the area of intelligent control of robotic systems including machine learning. He is a member of IEEE, JSME, CISE, ISCIE, and RSJ.